Identification of Unique Amino Acids That Modulate CYP4A7 Activity†

Patricia A. Loughran, Linda J. Roman, Alison E. Aitken, R. Timothy Miller,‡ and Bettie Sue S. Masters*

Department of Biochemistry, The University of Texas Health Science Center, 7703 Floyd Curl Drive, San Antonio, Texas 78229-3900

Received July 5, 2000; Revised Manuscript Received October 2, 2000

ABSTRACT: A multifamily sequence alignment of the rabbit CYP4A members with the known structure of CYP102 indicates amino acid differences falling within the so-called substrate recognition site(s) (SRS). Chimeric proteins constructed between CYP4A4 and CYP4A7 indicate that laurate activity is affected by the residues within SRS1 and prostaglandin activity is influenced by SRS2−3. Site-directed mutant proteins of CYP4A7 found laurate and arachidonate activity markedly diminished in the R90W mutant (SRS1) and somewhat decreased in W93S. While PGE_1 activity was only slightly increased, the mutant proteins H206Y and S255F (SRS2−3), on the other hand, exhibited remarkable increases in laurate and arachidonate metabolism (3-fold) above wild-type substrate metabolism. Mutant proteins H206Y, S255F, and H206Y/S255F but **not** R90W/W93S, wild-type CYP4A4, or CYP4A7 metabolized arachidonic acid in the absence of cytochrome b_5. Stopped-flow kinetic experiments were performed in a CO-saturated environment performed to estimate interaction rates of the monooxygenase reaction components. The mutant protein H206Y, which exhibits 3-fold higher than wild-type substrate activity, interacts with CPR at a rate at least 10 times faster than that of wild-type CYP4A7. These experimental results provide insight regarding the residues responsible for modulation of substrate specificity, affinity, and kinetics, as well as possible localization within the enzyme structure based on comparisons with homologous, known cytochrome P450 structures.

The number of cloned and sequenced cytochrome P450s (P450s) has been steadily increasing since the first cytochrome P450 was purified by Omura and Sato (*1*). The P450 superfamily now consists of 43 gene families comprised of >500 members, but the substrate specificities for only a minority of these are known (*2*). The CYP4A subfamily, which consists of eicosanoid- and fatty acid-metabolizing enzymes, is believed to play a role in the metabolism of arachidonic acid in lung, liver, and kidney (*3*−*6*). The mRNAs for these isoforms in rabbit have been characterized with respect to means of induction and tissue localization using RNase protection (RNAP) assays (*4, 7*−*9*). Substrate specificities were determined on protein produced in transiently transfected COS-1 cells (*4*). The specific aim of this paper is to ascertain the effects of mutating nonconserved residues of CYP4A7,[1] the only member of the CYP4A subfamily from rabbit kidney that can accommodate a prostaglandin as substrate (*3, 4, 10*). When considering the difference in size and shape of substrates for the CYP4A subfamily: laurate (12-carbon straight chain), prostaglandins (20-carbon, hairpin-shaped, unsaturated fatty acid chain containing a cyclopentane ring), and arachidonic acid (20-carbon, hairpin-shaped, unsaturated fatty acid chain), the active site of CYP4A7 must have remarkable flexibility compared to its CYP4A subfamily siblings (Scheme 1). By identifying and characterizing the residues that modulate substrate recognition and catalytic rates of CYP4A7, insight will be gained into the structural properties responsible for enzymatic function.

Negishi et al. (*11*) found, when screening mutants with steroids and other substrates of differing size, charge, or polarity, that the length of the chain most affected enzyme activity. Peterson's group has extensively characterized CYP102 (BM-3), a soluble bacterial P450. Of the 3D structures solved to date, CYP102 is the most functionally similar to the CYP4A family as it also catalyzes the hydroxylation of arachidonic and lauric acids. In their work on CYP102, Peterson's group found that mutagenesis within the active site at F87V resulted in the loss of catalytic activity due to greater lateral movement of the substrate with the loss of steric bulk at the bottom of the channel. Also, alterations in the charge of a key residue at the top of the channel (the mutation R47D) affected enzyme activity due to the inability to tether/capture the substrate for exposure to the heme center (*12*).

While these laboratories have produced definitive results with crystal structures, the intermediate step of using chimeric

† Supported by NIH Grant GM31296 to B.S.S.M.

* To whom correspondence should be addressed at the Department of Biochemistry-7760, The University of Texas Health Science Center, 7703 Floyd Curl Dr., San Antonio, TX 78229-3900.

‡ Present address: Graduate Center for Toxicology, University of Kentucky, 306 HSRB Chandler Medical Center, Lexington, KY 40536-0305.

[1] Abbreviations: 20-HETE, 20-hydroxyeicosatetraenoic acid (20-hydroxyarachidonic acid); AA, arachidonic acid; apo b_5, heme-depleted cytochrome b_5; b_5, cytochrome b_5; CD, circular dichroism; CPR, NADPH−cytochrome P450 reductase; CYP4A7, cytochrome P4504A7; DLPC, L-α-dilauroylphosphatidylcholine; IPTG, isopropyl β-D-thiogalactopyranoside; NP-40, Nonidet P-40; P4504A7, cytochrome P4504A7; $P450_{ka\text{-}2}$, cytochrome P4504A7; PGA_1, prostaglandin A_1; PGE_1, prostaglandin E_1; SDS−PAGE, sodium dodecyl sulfate−polyacrylamide gel electrophoresis; β-OG, β-octylglucoside; δ-ALA, δ-aminolevulinic acid.

10.1021/bi001522u CCC: $19.00 © 2000 American Chemical Society
Published on Web 11/14/2000

Scheme 1

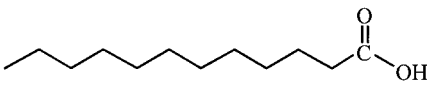

Lauric Acid

$C_{12}H_{24}O_2$

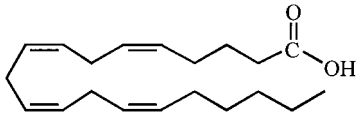

Arachidonic Acid

$C_{20}H_{34}O_2$

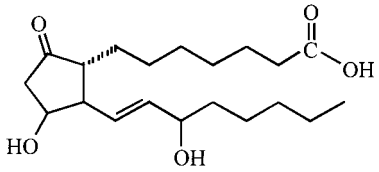

Prostaglandin E_1 (PGE_1)

$C_{20}H_{34}O_5$

proteins to localize areas involved in substrate specificities has been used in our study of CYP4A7. Previous work in our laboratory localized a 96-amino acid region involved in PGA_1, laurate, and arachidonic acid ω-hydroxylation using a CYP4A6/CYP4A4 chimera expressed in COS-1 cells (*13*). Comparison of the CYP4A6 and CYP4A4 sequences indicated that the ω-hydroxylation of these substrates was controlled by 10 amino acid differences, several of which were nonconservative, between CYP4A4 and CYP4A6. These amino acid differences were localized to the six SRSs previously described by Gotoh (*14*) and used successfully by Negishi in converting the substrate specificity of CYP2A4 to CYP2A5 from coumarin to testosterone (*11*). Further studies in our laboratory were discontinued because of low yields inherent in the COS-1 system. More recent work has employed expression in *E. coli*, a prokaryotic system, for kinetic and spectral characterization of rabbit CYP4A4, -5, and -7 (*15*−*18*). The focus of this paper was the identification of unique residues within CYP4A7 influencing enzymatic activity with various substrates. Our approach was to create chimeric proteins and site-directed mutant proteins, based on sequence alignment of the CYP4A members with the sequence of the crystallized, soluble bacterial P450, CYP102 (BM-3). By engineering chimeras between CYP4A4 and CYP4A7, it was possible to localize those residues influencing laurate (CYP4A7) and PGE_1 (CYP4A4) activity, which led to the construction of a number of site-directed mutations.

MATERIALS AND METHODS

The unlabeled fatty acid substrates (laurate, myristate, linoleate, oleate, and arachidonate) and L-α-dilauroylphosphatidylcholine (DLPC) were from Avanti. Radioactive substrates were obtained from Amersham. The unlabeled prostaglandin substrates (PGE_1 and PGA_1) were from Bio-Mol. Scintillation cocktail (Ultra Flow M) was from Packard. Restriction enzymes were from New England Biolabs. *Taq* DNA polymerase, T4 ligase, Transfast, and the Wizard Maxi preparatory DNA kit were purchased from Promega. T4 polynucleotide kinase was from GIBCO BRL/Life Technologies. The Quickchange Site-Directed Mutagenesis Kit was from Stratagene. Alexis was the source of isopropyl β-D-thiogalactopyranoside (IPTG), and δ-aminolevulinic acid (δ-ALA) came from Fluka. Yeast extract, tryptone, and bacto agar were from DIFCO. All other chemicals were of the highest grade available and were obtained from Sigma. The detergents, Nonidet P40 (NP-40) and β-octylglucoside (β-OG), were purchased from Calbiochem and Antarace Incorporated, respectively. Hydroxyapatite Bio-Gel HTP Gel was purchased from Bio Rad.

Plasmids. CYP17α and pCW were provided by Dr. Michael Waterman of Vanderbilt University in Nashville, TN. The cytochrome b_5 plasmid was provided by Dr. Ronald Estabrook of The University of Texas Southwestern Medical Center in Dallas, TX. The cytochrome P450 reductase plasmid was generously given by Dr. Charles Kasper of the University of Wisconsin in Madison, WI.

Recombinant DNA Manipulation. Successful expression of CYP4A7 was accomplished with the 17α4A7pCW construct. This construct contains the first 30 nucleotides from the cDNA of CYP17α, the first mammalian P450 to be expressed in *E. coli* (*19*). This was followed by the coding sequence for CYP4A7 minus the first 30 nucleotides. The 17α4A7pCW construct was created by restriction digestion of the sequence-confirmed 5′His4A7pCW and 17α4A6pCW constructs. The CYP4A7 coding sequence, previously subcloned in pSVL (*4*), was PCR-amplified, with the addition of the *Nde*I and *Hin*dIII restriction sites as well as the coding sequence for a 4-histidine track, to create the 5′His 4A7pCW construct.

The primers used were as follows:

A7pCW5: GG,ATA,TAA,CAT,ATG,GCT,CAC,CAC, CAC,CAC,CTG,AGC,TCC,ACC (upstream)

A7pCW4: GAA,GCT,TTA,GTG,GAG,CTT,CCT, GAG,AC (downstream)

Primers were synthesized by the Center for Advanced DNA Technologies at The University of Texas Health Science Center at San Antonio. Reaction mixtures included 50 pmol of each primer, 20 ng of CYP4A7 template, 0.5 mM $MgCl_2$, 0.1 mM dNTPs, 1×*Taq* DNA polymerase buffer, and 2.5 units of *Taq* DNA polymerase in 100 μL total volume. This mixture was preheated at 94 °C for 120 s prior to the addition of *Taq* DNA polymerase. Thirty cycles (94 °C for 60 s, 55 °C for 120 s, and 72 °C for 180 s) were performed. The PCR product was excised from a 1% agarose gel, and the DNA was extracted using the Gene Clean II kit (BIO101). The PCR product DNA was first subcloned into a PCR cloning pGem-T vector (Promega) with a T overhang and then removed via digestion with *Nde*I and *Hin*dIII to prepare the ends for ligation with pCW, which had also been restriction-digested. The 5′His4A7 PCR product with prepared ends, ligated with pCW (also with prepared ends), was transformed into SCS1 supercompetent cells (Stratagene), screened by restriction digestion, and then transformed into JM109 electrocompetent cells, resulting in the CYP4A7pCW construct.

The 17α4A6pCW was prepared as previously described (*20*). The CYP4A6 coding sequence, previously subcloned in pSVL (*4*), was PCR-amplified with the addition of the *Nde*I and *Hin*dIII restriction sites.

The primers used were the following:

5′A6: CGC,TGC,CAT,ATG, GCT,CTG, TTA, TTA, GCA,GTT,TTT,ACC,CGG,CTC,CCG,GGC (upstream)

3′A6: TCC,CCA,CAA,GCT,TTA,GCG,GAG,CTT, CCT,CAG,AC (downstream)

Following DNA sequencing confirmation of 5′His4A7pCW and 17α4A6pCW constructs, the 17α4A7pCW construct was created using these vectors. The 17α4A6pCW construct was restriction-digested with *Nde*I and *Xma*I, and the insert fragment was gel-isolated. The 5′His4A7pCW construct was restriction-digested with *Xma*I and *Hin*dIII, and the vector fragment was gel-isolated. The insert portion of 17α4A6pCW was ligated to the vector portion of 5′His4A7pCW. As the *Xma*I site begins at the end of the 10 amino acid addition of CYP17α, there is no CYP4A6 coding sequence in the 17α4A7pCW construct. The 17α4A7pCW construct was transformed into SCS1 supercompetent cells (Stratagene).

The CYP4A4 coding sequence, previously subcloned in pSVL by Roman et al. (*4*), was mutated by polymerase chain reaction (PCR) mutagenesis (*21*) at the N- and C-termini. At the N-terminus, amino acids 2, 3, and 4 were deleted and 5, 6, and 7 were codon-biased to the *E. coli*-preferred nucleotide sequences coding for the same amino acids. A 4-histidine residue tag was incorporated at the C-terminus by the addition of 3 histidines to the sequence. This modified CYP4A4 DNA was inserted into the pCW_{ori+} vector (*19*) by ligation of the *Nde*I/*Hind*III-cleaved vector and mutated CYP4A4 DNA.

The 17α4A7pCW construct was the base template for mutagenesis. Localization of substrate-specific residues relied on a multifamily sequence alignment of the rabbit CYP4A family to CYP102 using the Insight and Homology programs from BIOSYM performed on a Silicon Graphics Indigo 2 workstation. The alignment of the rabbit CYP4A family sequence to the structurally conserved secondary structure of CYP102 yielded highly positive Dayhoff's mutation matrix scores (*22*). Relevant portions of the multifamily alignment are labeled with the secondary structure portions of CYP102 as it aligns best with the entire coding sequence of the rabbit CYP4A family and its six SRS (Figure 1). This figure only displays the nonconserved differences localized within the SRS1−3 regions that were identified in the alignment of the rabbit CYP4A subfamily. Chimeric protein constructs were created by restriction digest (SRS1 = *Nde*I and *Sph*I; SRS2−3 = *Bam*HI and *Pst*I) and ligation to the analogous portions of CYP4A4 wild-type plasmid DNA (Figure 2). The hypothesized substrate profile of these regions is based on the characterization of CYP4A family members (*4*) and the knowledge that most CYP4A amino acid differences were within residues 65−120 and 170−240 (*3*).

The majority of site-directed mutations (R90W, W93S, R90W/W93S, and H206Y) were created by a three-primer method with the mutation residing in a phosphorylated mutant oligomer that is incorporated during PCR amplification (*27*). SRS1:

*Nde*17α: ATT,ATT,CAT,ATG,ATG,GCT,CTG,TTA, TTA,GCA,GTT,TTT,ACC,CGG,CCG,GGC, AGC,TTC,TCC (upstream)

3′*Sph*I: GGG,TGA,GCA,TGC,GCC (downstream)

R90W: GCC,TGT,CCT,**TGG**,TGG,CTG,TGG (mutant)

W93S: CGC,TGG,CTG,**AGT**,GGG,AGT,GAG (mutant)

R90W/W93S: GCC,TGT,CCT,**TGG**,TGG,CTG,**AGT**, GGG,AGT,GAG (mutant)

SRS2−3:

5′*Sph*I: ACC,GGC,GCA,TGC,TCA (upstream)

3′*Aat*II: GAG,GAG,GAC,GTC,CAG (downstream)

H206Y: GCC,TTC,AGC,**TAC**,CAG,GGC,AGC (mutant)

The mutant primers were phosphorylated in reactions containing 2 μg of mutant primer DNA, 5× forward buffer, T4 polymerase kinase, and 1 mM ATP, in 25 μL total volume. The samples were heated at 37 °C for 10 min; the reactions were quenched by heating at 65 °C for 10 min and were brought to a final volume of 75 μL. The mutagenesis reaction included 200 pmol of each primer, including the phosphorylated mutant oligo, 400 μM each dNTP, 1× ligase buffer, 5 units of polymerase, 40 units of *Taq* DNA ligase, and 20 ng (2×10^9 copies) of CYP17α4A7 template in 100 μL total volume. These reactions were preheated at 94 °C for 300 s, and at 55 °C for 60 s prior to the addition of *Taq* DNA polymerase and *Taq* DNA ligase. Thirty cycles (94 °C for 30 s, 55 °C for 60 s, and 65 °C for 240 s) were performed followed by one cycle of 94 °C for 30 s, 55 °C for 60 s, and 65 °C for 15 min (*27*). The PCR product was excised from a 1% agarose gel, and the DNA was extracted using the Gene Clean II kit (BIO101). The mutant 17α4A7 PCR product was restriction-digested with the appropriate restriction enzymes (*Nde*I and *Sph*I for SRS1 mutations and *Sph*I and *Aat*II for SRS2−3 mutations) to prepare its ends for ligation with the restriction-digested prepared ends of 17α4A7pCW. The mutant 17α4A7pCW constructs were transformed into SCS1 supercompetent cells (Stratagene), screened by restriction digest, and then transformed into JM109 via electroporation.

The mutant S255F was created using the QuikChange Site-Directed Mutagenesis Kit from Stratagene as follows:

5′255Kit: CCT,GAG,GGC,CGC,TTG,**TTT**,CAC,CGT, GCC,TGC,C (upstream)

3′255Kit: G,GCA,GGC,ACG,GTG,**AAA**,CAA,GCG, GCC,CTC,AGG (downstream)

The reaction mixtures contained 5 μL of 5× reaction buffer, 2 ng of CYP17α4A7 template, 125 ng of each primer, and 1 μL of dNTP mixture, to a volume of 49 μL. The reaction was heated at 95 °C for 30 s followed by the addition of 1 μL of *Pfu* Turbo polymerase, to a final volume of 50 μL.

The reaction was then heated at 95 °C for 30 s, followed by 16 cycles of 95 °C for 30 s, 55 °C for 1 min, and 68 °C for 13 min. The PCR reaction was run on a 1% agarose gel to confirm the PCR product. The restriction enzyme *Dpn*I (1 μL) was added to 10 μL of the PCR reaction and heated at 37 °C for 18 h. One microliter of the *Dpn*I-treated PCR reaction was used to transform 50 μL of XL-1 blue cells (Stratagene).

The mutant protein H206Y/S255F was created as a chimera. The cDNAs of H206Y and S255F were restriction-digested with the enzymes *Sac*I and *Hin*dIII. The insert fragment of S255F and the vector portion of H206Y were gel-isolated and ligated. The double mutant H206Y/S255F ligation product was then transformed into SCS1 supercompetent cells (Stratagene).

All transformation reactions were plated on LB/ampicillin (50 μg/mL) plates. Proper insertion/orientation of the insert in the vector was confirmed by restriction digest of plasmid isolated using the standard alkaline lysis minipreparation. DNA from SCS1 or XL-1 positive colonies was transformed into JM109 competent cells for protein expression in bacteria. The sequences of all cDNA constructs were confirmed by the Center for Advanced DNA Technologies, The University of Texas Health Science Center at San Antonio.

Protein Expression. A preparation of CYP4A7 wild type, CYP4A4 wild type, and variants were expressed and purified as previously described (*17*, *18*). Fernbach flasks containing 750 mL of Modified Terrific Broth (20 g of yeast extract, 10 g of bactotryptone, 2.65 g of KH_2PO_4, 4.33 g of Na_2PO_4, and 4 mL of glycerol) and 50 μg/mL ampicillin were inoculated with 0.75 mL of an overnight culture (3 mL of LB + 50 μg/mL ampicillin) and shaken at 250 rpm at 37 °C. CYP protein expression was induced at $OD_{600} = 1.0$ with 0.5 mM IPTG. Cultures were simultaneously supplemented with 225 μM δ-aminolevulinic acid (δ-ALA), a precursor of heme biosynthesis. The flasks were shaken at 250 rpm at 37 °C for an additional 18 h. The cells were harvested by centrifugation, and the cell paste was frozen at −20 °C until purification (*28*).

Protein Purification. Harvested cells were resuspended in 50 mL of resuspension buffer (100 mM Tris-HCl, pH 7.4, 1 mM EDTA, 20% glycerol) and were lysed by pulsed sonication (6 min, 60% power, small probe). Cell debris was removed by ultracentrifugation at 44000*g* for 70 min. The crude protein was solubilized in KPO_4 solubilization buffer (20 mM KPO_4, pH 7.4, 10% glycerol, 0.3% NP-40) by resuspending the pellet in 30 mL of KPO_4 solubilization buffer and homogenizing with a Potter−Elvehjem tissue grinder. The homogenate was gently stirred overnight at 4 °C. Cellular debris was removed by ultracentrifugation at 36500*g* for 70 min.

The CYP4A7 supernatant was then applied to a 5 mL, 1.5 cm hydroxylapatite column (BioRad), which had been pre-equilibrated with 10× column volumes of KPO_4 solubilization buffer. The protein-loaded column was washed with 10× column volumes of KPO_4 solubilization buffer and then with 3× column volumes in KPO_4 elution buffer (20 mM KPO_4, pH 7.4, 10% glycerol, 25 mM β-OG) in order to switch detergents. The enzyme was eluted from the column with the addition of KPO_4 elution buffer, concentrated, dialyzed in KPO_4 dialysis buffer (20 mM KPO_4, pH 7.4, 0.5 mM EDTA, pH 8.0, 25 mM NaCl, 10% glycerol), and stored at −80 °C in 150 μL aliquots.

The CYP4A4 purification involved the addition of a small volume of 5 M NaCl to the membrane-solubilized supernatant to bring the salt concentration to 50 mM NaCl. The membrane-solubilized supernatant was loaded onto a DE53 column, which had previously been equilibrated in KPO_4 solubilization buffer (20 mM KPO_4, pH 7.4, with 10% glycerol, 0.3% NP-40, and 25 mM NaCl). The flow-through, which contained the CYP4A4, was collected. A small volume of KPO_4 solubilization buffer (2× the column volume) was also washed through the DE53 column to remove any remaining CYP4A4. The flow-through and short wash were loaded onto a small nickel-chelating column (Qiagen nickel-chelating agarose). The column was then subjected to three different wash steps. First, 50 mL of nickel column wash buffer (20 mM KPO_4, pH 7.4, with 10% glycerol, 0.3% NP-40, and 250 mM NaCl) followed by 50 mL of the same buffer plus 1 mM histidine was applied. Finally, 30 mL of nickel column wash buffer (20 mM KPO_4, pH 7.4, with 10% glycerol, 25 mM β-OG, and 250 mM NaCl) was applied to exchange the non-dialyzable detergent, NP-40, for the easily dialyzable alternative, β-OG. CYP4A4 was eluted from the nickel column in CYP4A4 elution buffer (20 mM KPO_4, pH 7.4, with 10% glycerol, 25 mM β-OG, 250 mM NaCl, and 20 mM histidine). Fractions were collected and screened by SDS−PAGE electrophoresis before pooling. Fractions containing CYP4A4 only were pooled and dialyzed against CYP4A4 dialysis buffer (20 mM KPO_4, pH 7.4, with 10% glycerol and 100 mM NaCl) (*17*).

The mutant constructs were expressed in *E. coli* and purified, having been eluted from a hydroxylapatite column in the detergent β-octylglucoside essentially the same as wild type. The mutant proteins and wild-type CYP4A7 were purified only by hydroxylapatite column chromatography as the protein did not bind to a variety of other column materials. The mutant proteins, R90W, W93S, R90W/W93S, and H206Y/S255F, precipitate on dialysis. Samples were removed from dialysis, the precipitated protein was pelleted, and the heme content of the remaining supernatant containing soluble cytochrome P450 was measured by CO-difference spectroscopy (data not shown). Because of protein instability, assay optimization studies were performed. The mutant W93R and wild-type CYP4A7 were assayed at the membrane-solubilized stage, in case heme instability was exacerbated by column purification. The activity of the W93R mutant was further reduced when examined at the membrane-solubilized stage. This minimization of substrate metabolism by the mutant enzyme is most likely the result of protein degradation caused by increased levels of proteases acting on an unstable mutant protein. Wild-type protein exhibited comparable activity at the solubilized cell stage to that of the purified protein. These results indicated the need to stabilize the mutant proteins that precipitated during dialysis to achieve a credible characterization of substrate specificity. The roles of detergent (β-OG) and salt (NaCl) were examined in hopes that they would act to stabilize the unstable mutants. Substrate metabolism levels were highest in the presence of β-OG (25 mM) and NaCl (25 mM), yet the unstable mutant proteins would precipitate in the process of reducing the salt concentration. Therefore, it was decided to store the unstable mutant proteins, R90W, W93S, R90W/W93S, and H206Y/

S255F, in the presence of 25 mM β-OG and 1 M NaCl and characterize the entire set of proteins at constant detergent and salt levels within the reconstitution assay. A control experiment using a range of arachidonic acid concentrations and wild-type protein with detergent and NaCl added was performed to confirm saturation kinetics (data not shown).

The concentrations of enzymes were determined by reduced, CO-difference spectra to detect the presence of heme-containing proteins. Although this method underestimates the amount of protein, it accurately determines the amount of heme-containing cytochrome P450 due to its unique reduced, CO-difference spectral signature at ~450 nm. The level of homogeneity of the preparation was determined by Bradford assay (*29*), SDS−PAGE electrophoresis, and immunoblot analysis (data not presented).

Preparation of NADPH−Cytochrome P450 Reductase (CPR). CPR was expressed and purified as described (*30*, *31*) for use in reconstitution experiments. The concentration of flavin-containing protein was calculated from the absorbance at 454 nm using an extinction coefficient of 20.16 mM^{-1} cm^{-1} for the flavin content of 2 flavins per mole of CPR (10.08 mM^{-1} cm^{-1} per flavin).

Preparation of Cytochrome b_5 and Heme-Depleted Cytochrome b_5 (Apo b_5). Rat microsomal cytochrome b_5 was expressed in *E. coli*, and protein was purified according to Holmans et al. (*32*). The concentration of apo- and holoprotein was calculated from the absorbance at 413 nm using an extinction coefficient of 117 mM^{-1} cm^{-1} (*33*). Heme-depleted cytochrome b_5 was prepared as described by Cinti and Ozols (*34*).

Spectrophotometric Methods. Reduced, CO-difference spectra were obtained by reducing the protein with dithionite and then bubbling the sample with CO. The spectrum was recorded from 400 to 500 nm. The concentration of spectrally intact cytochrome P450 was determined using the extinction coefficient of 91 mM^{-1} cm^{-1} for the difference in absorbance between 450 and 490 nm (*1*).

Activity Assays. The ω-hydroxylation of substrate was assayed in reaction mixtures containing purified CYP, DLPC, and CPR in the presence or absence of cytochrome b_5 as specifically described in the figure legends. The reactions were initiated by the addition of isocitrate, isocitrate dehydrogenase, and NADPH. The conversion of substrate to the ω-hydroxylated product was measured on a C18 column with a Beckman System Gold HLPC equipped with an online radioisotope flow detector. Data are expressed as the mean ± standard deviation of triplicate determinations obtained from two to three independent experiments. Data were analyzed by the Hanes−Woolf plot (*35*).

Stopped-Flow Spectrophotometry. Purified CYP4A7, H206Y, CPR, cytochrome b_5, and apo cytochrome b_5 were diluted in reaction buffer (20 mM KPO_4, pH 7.4, 0.5 mM EDTA, 25 mM NaCl, 10% glycerol) to final protein concentrations of 1.0 μM CYP4A7, 1.0 μM H206Y, 1.0 μM CPR, 2.0 μM cytochrome b_5, or 2.0 μM apo cytochrome b_5. The detergent DLPC (5 μg/mL) was present in the reactions to maintain optimal assay conditions. CYP4A7's primary substrate laurate (100 μM) was evaporated under nitrogen to remove methanol and was resuspended by the assay components in order of addition established for optimal assay activity. Stopped-flow spectra were measured at room temperature under CO-saturating conditions (*36*, *37*). NADPH (200 μM)-initiated P450, cytochrome b_5 heme, or CPR flavin reduction was monitored at 449 nm (H206Y), 451 nm (CYP4A7), 424 nm (cytochrome b_5 and apo cytochrome b_5), or 390 nm (flavin), respectively. The kinetic traces were collected on an Applied Photophysics SX 18MV microvolume stopped-flow reaction analyzer (Applied Photophysics, Leatherhead, U.K.). The data presented are an average of a minimum of 5−11 kinetic traces. A single-exponential equation was applied separately to both the flavin reduction and heme reduction of the above traces using the manufacturer's software package [single exponential with the steady-state formula: $P(1)$ *exp(−$P(2)$*X) + $P(3)$*X + $P(4)$, where $P(1)$ = amplitude, $P(2)$ = rate, $P(3)$ = slope, and $P(4)$ = intercept; Applied Photophysics Software SX18MV, v4.38]. The residuals for each experiment are displayed below their respective kinetic traces (*38*).

RESULTS

A multifamily sequence alignment confirmed the earlier observation (*3*, *4*) that the majority of differences among the rabbit CYP4A subfamily members fall within distinct regions. We have indicated regions of conserved secondary structure and SRS(s) in the pertinent regions of interest (Materials and Methods) (Figure 1). Based on the sequence alignment, previous work with chimeras of CYP4A4 and CYP4A6 (*13*), and known substrate profile differences among the individual CYP4A members (*4*), predictions of substrate activities with various substrates in the SRS1, -2, and -3 regions were made (Figure 2). Chimeric proteins of CYP4A4 and CYP4A7 were created by restriction digest and ligation to clarify the roles of four nonconserved amino acids (90, 93, 206, and 255) of CYP4A4 and CYP4A7 (Figure 2). ω-Hydroxylation of laurate, arachidonic acid, and PGE_1 was measured as described under Materials and Methods. The expression and enzymatic activity of the chimeras were lower than those of wild type, although they exhibit sufficient enzymatic activity to conclude that those residues affecting substrate turnover have been identified (Figure 3). Comparison of known substrate differences between CYP4A7 and CYP4A4 in combination with the results from the chimeric proteins led to the selection of nonconserved amino acid differences at residues 90, 93, 206, and 255 for site-directed mutagenesis (Table 1). In addition to these single point mutations, two double mutants, R90W/W93S and H206Y/S255F, were created in order to distinguish between their respective single mutants for a definitive localization of substrate-modulating residues. The data shown in Table 2 demonstrate that mutations in the SRS1 region, i.e., R90W, W93S, and R90W/W93S, decrease both laurate and arachidonate hydroxylation, albeit to different degrees. In 4A7wt (CYP4A7), the ratio of laurate activity to that of arachidonate is about 1:1, while that of 4A4wt (CYP4A4) is about 1:7. The R90W mutation causes the substrate profile of CYP4A7 to more closely resemble that of CYP4A4; the ratio of laurate activity to that of arachidonate is 1:6. The W93S and R90W/W93S mutants, on the other hand, more closely resemble their parent CYP4A7; laurate:arachidonate is about 1:1 in either case. The mutations in the SRS2−3 region all increase both laurate and arachidonate hydroxylation by approximately 3-fold. The ratio of laurate hydroxylation to that of arachidonate, however, is 1:1 in all cases. Thus, the substrate

```
                       B            SRS-1                       C
CYP102   :       KIA-DELGEIFKFEA-PGRVTRYLS--------SQRLIKEACDE-SRFDK
CYP108   :       WLR-DEQ-PLAMAHIEGYDPMWIAT--------KHADVMQIGKQPGLFSN
CYP101   :       VLG-ES-NVPDLVWTRCNGGHWIAT--------RGQLIREAYEDYRHFSS
CYP17    :       KLQEKYG-PIYSFRL-GSKTTVMIGHHQ-L--AREVLLKKGKEFSGRP--
CYP11A1  :       NFQ-KYG-PIYREKL-GNLESVYIIHPE----DVAHLFKFEGSYPERYDI
CYP4A4   :   75  ERIQKW---VEKFPG--ACPWWLSGNKARLLVYDPDYLKVIL---GRSDP  116
CYP4A5   :       QQILKW---VEKFPR--ACPHWIGGNKVRVQLYDPDYMKVIL---GRSDP
CYP4A6   :       VML-KW---VEKFPS--ACPRWLWGSRAHLLIYDPDYMKVIL---GRSDP
CYP4A7   :   75  QVL-KR---VEKFPS--ACPRWLWGSELFLICYDPDYMKTIL---GRSDP  116
                 F     SRS-2
CYP102   :       IGLCGNYRFFNSFYR--DQPH--PFITSMVRALDEAMNKLQRANPDDPAY
CYP108   :       VVMTAL----G------VPEDDEPLMLKLTQDFFGV-------------
CYP101   :       IFMLLA----G------LPEEDIPHLKYLTDQMTRP-------------
CYP17    :       TNIISFICFNF------SFKNEDPALKAIQNVNDGILEVLSKEVLLDIFP
CYP11A1  :       ITNVMF-GERLGMLEETVNPEAQKFIDAVYKMFHTSV-PLLNVPPELYRL
CYP4A4   :  199  IMKCAF------SYQGSVQLD--RNSHSYIQAINDLNNLVFYRARNVFHQ  240
CYP4A5   :       IMKCAF------SYQGSVQLD-SRNSQSYIQAVGDLNNLVFARVRNIFHQ
CYP4A6   :       IMKCAF------SHQGSVQLD--RNSQSYIQAVGDLNNLFFSRVRNVFHQ
CYP4A7   :  199  IMKCAR------SHQGSVQLE-SRTSKSYIQAVRELSDLALQRVRNVFHQ  240
                              SRS-3      G              H
CYP102   :       --------DENKRQFQEDIKVMNDLVDKIIADRK--ASGEQSDDLLTHML
CYP108   :       ---------EAARRFHETIATFYDYFNGFTVDRR----SCPKDDVMSLLA
CYP101   :       ---------DGSMTFAEAKEALYDYLIPIIEQRR----QKPGTDAISIVA
CYP17    :       VLKIFP--SKAMEKMKGCVQTRNELLNEILEKCQENFSSDSITNLLHILI
CYP11A1  :       FRTKTW--RDHVAAWDTIFNKAEKYTEIFYQDLR----RKTEFRNYPGIL
CYP4A4   :  241  SDFL-YRLSPEGRLFHRACQLAHEHTDRVIQQRK---AQLQQEGELEKVR  286
CYP4A5   :       SDTI-YRLSPEGRLSHRACQLAHEHTDRVIQQRK---AQLQQEGELEKVR
CYP4A6   :       SDTI-YRLSPEGRLSHRACQLAHEHTDRVIQQRK---AQLQQEGELEKVR
CYP4A7   :  241  SDFL-YRLSPEGRLSHRACQLAHEHTDRVIQQRK---AQLQQEGELEKVR  287
```

FIGURE 1: Determination of regions that determine CYP4A7 substrate specificity. Localizing possible substrate sites begins with the use of sequence alignment of the CYP4A members to the bacterial P450s (CYP102, CYP101, CYP103) which have been crystallized (*23*−*25*). These three-dimensional structures all have the same basic core structure surrounding the heme (*26*). While the bacterial CYPs are smaller than mammalian P450s, structural feature/CYP4A7 framework can be obtained by a group-to-group comparison through alignment of the α helices. The letters B, C, F, G, and H refer to the B, C, F, G, and H α helices. The designation SRS-1, -2, and -3 refers to the substrate recognition site(s) 1, 2, and 3 (*14*).

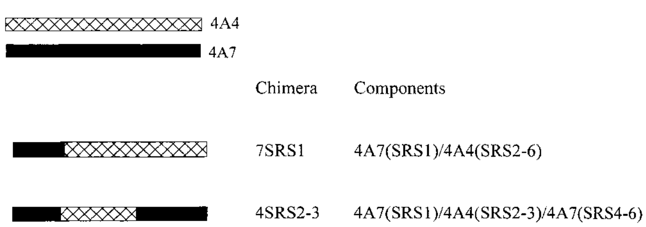

Substrate Recognition Site (SRS)	CYP4A7 Residue	Secondary Structure in CYP102
1	86-109	β1(2) sheet
2	200-209	F alpha helix
3	252-258	G alpha helix
4	295-319	I alpha helix
5	383-398	β1(4) sheet
6	488-498	β3(2) sheet

FIGURE 2: Localization of pertinent SRS. The regions of CYP4A4 and CYP4A7 to be combined were chosen based on group-to-group sequence alignment of the rabbit 4A members with the sequences of the crystallized CYP102 and information from chimeric constructs of CYP4A6/CYP4A4 (*13*). Chimeras were created by restriction digest and ligation.

profiles of these mutant enzymes are very similar to that of the parent CYP4A7.

Other studies showed that cytochrome b_5 or heme-depleted cytochrome b_5 improved product formation (*18*). This increase in enzyme activity by cytochrome b_5 is the result of a conformational change and not electron transfer, as increased activity is still present with heme-depleted cyto-

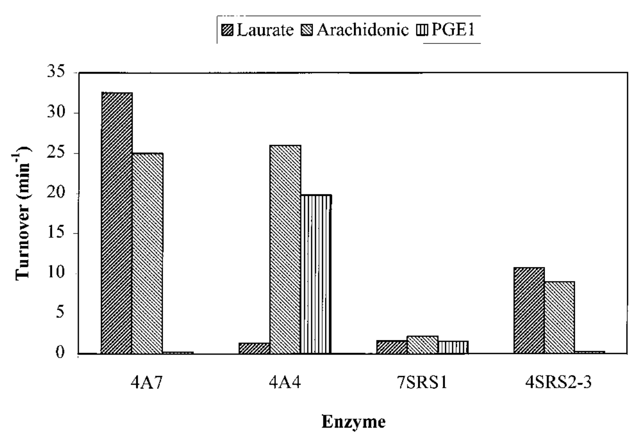

FIGURE 3: Determination of substrate specificity conferred by SRS1 and SRS2−3. The SRS1 regions of 4A4 and 4A7 were restriction-digested and ligated into the remaining portion of the other isoform examined. Chimeric proteins were expressed in *E. coli* and purified, having been eluted from a hydroxylapatite column in the detergent β-octylglucoside. The ω-hydroxylation of substrate was assayed in reaction mixtures containing purified wild-type protein (50 nM) or chimeric protein (100 nM), the lipid L-α-dilauroylphosphatidylcholine (DLPC), NADPH−cytochrome P450 reductase, and cytochrome b_5. The reactions were initiated by the addition of isocitrate, isocitrate dehydrogenase, and NADPH in a regenerating system. The conversion of substrate to the ω-hydroxylated product was measured on a C18 column with a Beckman System Gold HLPC equipped with an online radioisotope flow detector.

Table 1: Proposed Substrate-Specific Residues of CYP4A7[a]

mutant	4A7	4A4	secondary structure	SRS
R90W	Arg	Trp	β1(2) sheet	1
W93S	Trp	Ser	β1(2) sheet	1
H206Y	His	Tyr	F α helix	2
S255F	Ser	Phe	G α helix	3

[a] The residues of CYP4A7 to be mutated have been chosen based on amino acid sequence alignment of the CYP4A members with the sequences of the crystallized CYP102 (BM-3) and information derived from the activities of chimeric constructs.

Table 2: Determination of Substrate Specificities of CYP4A7[a]

residue	turnover (min^{-1})			laurate: arachidonate ratio
	laurate	arachidonate	PGE_1	
4A7wt	46 ± 2.2	43 ± 2.9	11 ± 1.1	1:1
4A4wt	7 ± 0.5	47 ± 6.3	23 ± 2	1:7
R90W	1.6 ± 0.6	10 ± 2.4	17 ± 0.1	1:6
W93S	30 ± 2.7	27 ± 2.3	18 ± 0.5	~1:1
R90W/W93S	12 ± 0.3	13 ± 1.2	15 ± 1.0	~1:1
H206Y	134 ± 5.9	140 ± 7.4	25 ± 0.6	~1:1
S255F	160 ± 6.6	129 ± 7.8	18 ± 1	~1:1
H206Y/S255F	147 ± 5.0	130 ± 2.6	18 ± 0.7	~1:1

[a] The ω-hydroxylation of substrate (50 μM) was assayed in reaction mixtures containing purified wild-type protein (50 nM) or site-directed mutant protein (50 nM), the lipid L-α-dilauroylphosphatidylcholine (DLPC, 10 μg), NADPH−cytochrome P450 reductase (63 nM), and cytochrome b_5 (100 nM). The final concentration of detergent and salt is 1.5 mM β-OG, 60 mM NaCl in the reaction mixtures. The reactions were initiated by the addition of isocitrate, isocitrate dehydrogenase, and NADPH in a regenerating system. The conversion of substrate to the ω-hydroxylated product was measured on a C18 column with a Beckman System Gold HLPC equipped with an online radioisotope flow detector. Data are expressed as the mean ± standard deviation of triplicate determinations obtained from three independent experiments.

chrome b_5, which is unable to transfer electrons. As wild-type CYP4A7 and CYP4A4 proteins show no metabolism of arachidonic acid in the absence of cytochrome b_5 or heme-depleted cytochrome b_5, the ability of the mutant proteins of SRS2−3 to form ω-hydroxylated arachidonic acid in the absence of cytochrome b_5 was examined. Mutants H206Y, S255F, and H206Y/S255F, but not R90W/W93R, metabolized arachidonic acid in the absence of cytochrome b_5 (Table 3), albeit at low rates.

Because mutant proteins of the SRS2−3 region are able to metabolize arachidonate in the absence of cytochrome b_5 and possess greater than wild-type activity, differences in the rate of flavin and heme reduction were investigated using stopped-flow spectrophotometry. Our purpose was to determine if this increased activity was the result of greater catalytic efficiency. Having established by steady-state kinetics that the presence of cytochrome b_5 improves CYP4A7's catalytic efficiency but not substrate affinity (*18*), stopped-flow kinetic experiments were performed in a CO-saturated environment. This isolation of the first electron donation step of the monooxygenase reaction permitted estimations of interaction rates of the monooxygenase reaction components. Comparisons show that the flavin reduction phase (fast phase) of the wild-type CYP4A7 monooxygenase reaction is not altered in the presence or absence of cytochrome b_5 (Table 4). NADPH reduction of CPR is not obviously affected until we focus on the mutant H206Y. Flavin reduction (fast phase) is decreased in the presence of cytochrome b_5 or apo cytochrome b_5 when

Table 3: Determination of Arachidonic Acid Activity in the Presence and Absence of Cytochrome b_5[a]

sample	cytochrome b_5	turnover (min^{-1})
4A7wt	+	43 ± 2.9
	−	nd[b]
4A4wt	+	47 ± 6.3
	−	nd
R90W/W93S	+	13 ± 1.2
	−	nd
H206Y	+	140 ± 7.4
	−	4 ± 1.5
S255F	+	129 ± 7.8
	−	6 ± 1.8
H206Y/S255F	+	129 ± 2.6
	−	12 ± 1.9

[a] The ω-hydroxylation of arachidonic acid was assayed in reaction mixtures containing purified wild-type protein (50 nM) or site-directed mutant protein (50 nM), the lipid L-α-dilauroylphosphatidylcholine (DLPC, 10 μg), NADPH−cytochrome P450 reductase (63 nM), and cytochrome b_5 (100 nM). The final concentration of detergent and salt is 1.5 mM β-OG, 60 mM NaCl in the reaction mixtures. The reactions were initiated by the addition of isocitrate, isocitrate dehydrogenase, and NADPH in a regenerating system. The conversion of substrate to the ω-hydroxylated product was measured on a C18 column with a Beckman System Gold HLPC equipped with an online radioisotope flow detector. Data are expressed as the mean ± standard deviation of triplicate determinations obtained from two independent experiments. [b] nd: not detectable.

Table 4: Comparison of Rates of CYP4A7 or H206Y Heme Reduction in the Presence and Absence of Cytochrome b_5 or Apo Cytochrome b_5[a]

sample	4A7 (451 nm)		H206Y (449 nm)	
	fast phase (s^{-1})	slow phase (s^{-1})	fast phase (s^{-1})	slow phase (s^{-1})
CYP	87.1	6.9	71.8	7.6
CYP+cyt b_5	91.7	9.0	56.2	4.4
CYP+apo b_5	91.7	10.7	39.8	7.0

[a] The heme reduction of wild-type and mutant protein was measured at 451 and 449 nm, respectively. The control measurements were followed at 390 nm for the CPR sample alone, and at 424 nm for samples containing cytochrome or apo cytochrome b_5. The fast phase (flavin reduction) value was determined from 0 to 0.05 s, and the slow phase (heme reduction) was measured from 0.05 to 1 s of the same sample trace. The traces (a minimum of 5−11) of each sample are fit independently to a single exponential with steady-state formula. All samples were added to 100 μM laurate that had been dried down under N_2 gas in a silanized glass reaction tube. The ratios of added components and their order of addition (1:1 CPR to CYP4A7, 5 μg/mL DLPC, and 2:1 cytochrome b_5 or apo b_5 to CYP4A7) were consistent with previously established conditions.

complexed with the mutant cytochrome P450. Heme reduction (slow phase) of wild-type 4A7 is slightly enhanced in the presence of cytochrome b_5, but is reduced in the mutant H206Y (Table 4 and Figure 4). The mutant protein H206Y, which exhibited a 3-fold higher than wild-type substrate hydroxylation, exhibits a 10-fold higher rate of CPR interaction (the lower limit for the rate of binding that must occur prior to electron transfer) than that of wild-type CYP4A7. The rate of cytochrome b_5 binding under similar constraints is comparable for H206Y and wild-type protein (Table 5, Figure 5). There is a 30-fold higher rate of cytochrome b_5 interaction with wild-type CYP4A7 versus the rate of CPR interaction. A similar comparison of the rate of redox component interaction with the mutant protein H206Y indicates a 3-fold higher rate of cytochrome b_5 versus CPR interaction.

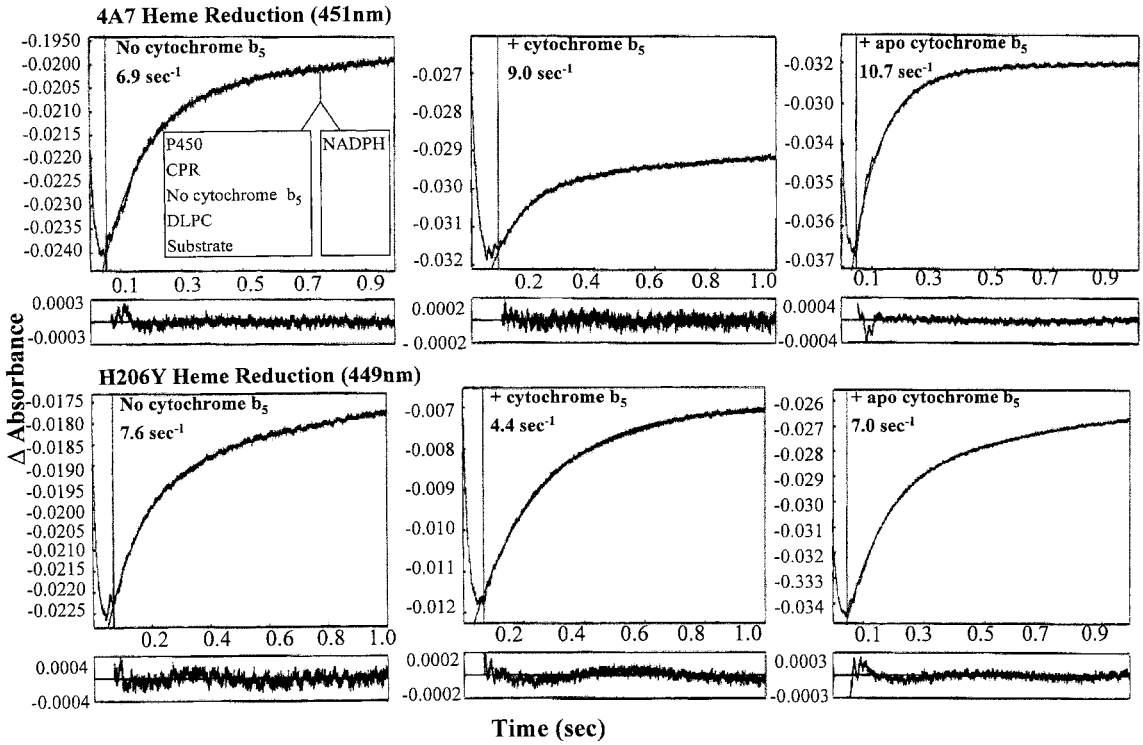

FIGURE 4: Estimation of the rate of heme reduction of CYP4A7 and CYP4A7H206Y in the absence and presence of cytochrome b_5 or apo cytochrome b_5. The ratios of added components and their order of addition (1:1 CPR to CYP4A7, 5 μg/mL DLPC, and 2:1 cytochrome b_5 or apo b_5 to CYP4A7) were consistent with previously established conditions (Materials and Methods). The estimated rate of heme reduction was determined with 1.0 μM 4A7 or 1.0 μM H206Y, 1.0 μM CPR, 2.0 μM cytochrome b_5, 100 μM laurate, and buffer in one syringe with the second syringe containing 200 μM NADPH. The traces (a minimum of 5−11) of each sample are fit independently to a single exponential with steady-state formula.

Table 5: Comparison of CYP4A7 and H206Y Rates of Interaction with CPR or Cytochrome b_5[a]

sample	CPR rate of interaction (s^{-1})	cytochrome b_5 rate of interaction (s^{-1})
$4A7_{(451\ nm)}$	0.3	9.1
$H206Y_{(449\ nm)}$	2.6	7.7

[a] The heme reduction of wild-type and mutant protein was measured at 451 and 449 nm, respectively. CPR binding rate was estimated by having 1.0 μM 4A7 or 1.0 μM H206Y, 2.0 μM cytochrome b_5, 100 μM laurate, and buffer in one syringe with the second syringe containing 1.0 μM CPR and 200 μM NADPH. The estimated rate of cytochrome b_5 binding was determined with 1.0 μM 4A7 or 1.0 μM H206Y, 1.0 μM CPR, 100 μM laurate, and buffer in one syringe with the second syringe containing 2.0 μM cytochrome b_5 and 200 μM NADPH. The traces (a minimum of 5−11) of each sample are fit independently to a single exponential with steady-state formula. All samples were added to 100 μM laurate that had been dried down under N_2 gas in a silanized glass reaction tube. The ratios of added components and their order of addition (1:1 CPR to CYP4A7, 5 μg/mL DLPC, and 2:1 cytochrome b_5 or apo b_5 to CYP4A7) were consistent with previously established conditions.

DISCUSSION

To determine which residues affect CYP4A7 substrate turnover, chimeric proteins and site-directed mutant proteins were created. The regions of CYP4A7 and CYP4A4 to be combined were chosen based on sequence alignment of the CYP4A members with the sequence of the crystallized, soluble bacterial P450, CYP102. This technique has been used successfully to identify residues that determine substrate specificity in other P450 isoforms (*11, 14, 39*−*42*). Chimeras were engineered with CYP4A4 and CYP4A7 to differentiate between these highly sequence-identical isozymes, and they allowed for identification of regions of the protein involved in laurate, arachidonate, and PGE_1 metabolism. These studies agreed with work in COS-1 cells in demonstrating that a 96-amino acid region within the middle third of the protein is involved in PGE_1, laurate, and arachidonic acid ω-hydroxylation (*13*). The four nonconserved amino acids highlighted by sequence alignments of the CYP4A subfamily are localized within or bordering SRS1, -2, and -3. The engineering of the SRS1, β1 sheet region, of CYP4A7 into CYP4A4 increased laurate activity to levels greater than wild-type CYP4A4. Likewise, the reciprocal chimera diminished laurate activity levels significantly below wild-type CYP4A7.

To further localize which nonconserved residues of CYP4A7 influence product formation, site-directed studies were initiated. Residues in CYP4A7 were mutated to the corresponding residues in CYP4A4. The putative localization of R90W and W93S at the top of the active site channel would suggest that these residues act as substrate anchors for proper insertion into the active site, as found in CYP102 metabolism of arachidonic acid (*12*). Laurate activity was diminished by 96% in R90W and by 35% in W93S. The intermediate turnover rate of laurate metabolism in the double mutant R90W/W93S is diminished by 74%, suggesting that the side chain of amino acid 90 is more accessible to the substrate and functions to tether the substrate at the appropriate distance from the reactive $Fe^{2+}-O_2$ for terminal carbon hydroxylation (*24*). In addition to the possibility of a direct interaction role in substrate metabolism, these two residues are also localized within the putative CPR binding region (*43*−*45*) and the overlapping cytochrome b_5 binding regions (*46*) at the top of the active site channel of the

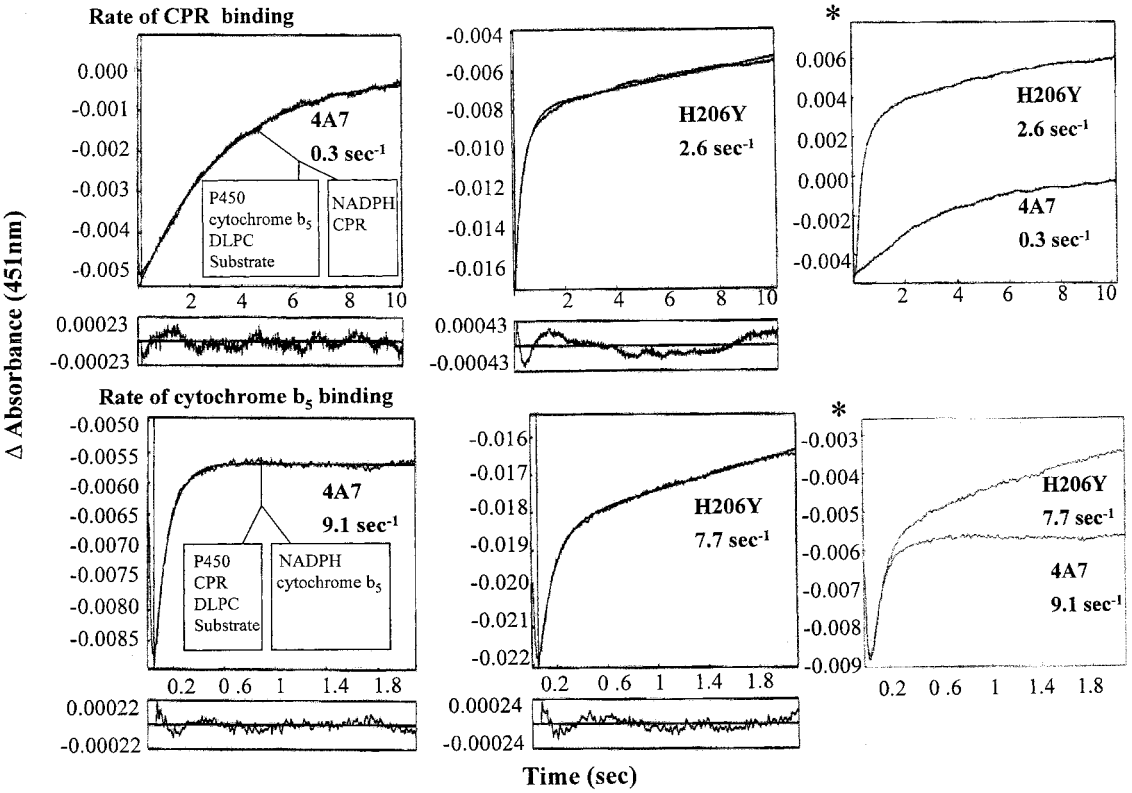

FIGURE 5: Estimation of the rate of CPR or cytochrome b_5 interaction with CYP4A7 or CYP4A7H206Y. The ratios of added components and their order of addition (1:1 CPR to CYP4A7, 5 μg/mL DLPC, and 2:1 cytochrome b_5 or apo b_5 to CYP4A7) were consistent with previously established conditions (Materials and Methods). The heme reduction of wild type and mutant protein was measured at 451 and 449 nm, respectively. CPR binding rate was estimated by having 1.0 μM 4A7 or 1.0 μM H206Y, 2.0 μM cytochrome b_5, 100 μM laurate, and buffer in one syringe with the second syringe containing 1.0 μM CPR and 200 μM NADPH. The estimated rate of cytochrome b_5 binding was determined with 1.0 μM 4A7 or 1.0 μM H206Y, 1.0 μM CPR, 100 μM laurate, and buffer in one syringe with the second syringe containing 2.0 μM cytochrome b_5 and 200 μM NADPH. The traces (a minimum of 5−11) of each sample are fit independently to a single exponential with steady-state formula.

proximal surface. Thus, the binding of these two important constituents of the monooxygenase reaction may also have been impacted by our alteration of these residues. This would be reflected in the low overall enzymatic activity for all three substrates examined. Additional experiments were not performed due to limiting amounts of mutant (R90W and W93S) enzymes.

The SRS2−3 region, which is localized to the F and G α helices, contains residues involved in arachidonate and prostaglandin activity, a conclusion based upon chimeric constructs, substrate profile, and amino acid differences of the CYP4A subfamily (*3, 4*). Earlier characterization of CYP4A4 and CYP4A7 showed that arachidonate is metabolized at comparable levels by the two isoforms, with comparable K_m and subsequent catalytic efficiency (*18, 47*). Arachidonate metabolism by CYP4A4 is surpassed by its preferred substrate, PGE_1, also based on catalytic efficiency and K_m values (*47*). The subtle differences in turnover numbers and K_m values for arachidonate and the significant differences in those values for PGE_1, which are altered by the mutation of two nonconserved amino acids within the SRS2−3 region (H206Y and S255F), reflect the ability of bulky and nonpolar residues to influence the orientation of a substrate and binding to the residues lining the active site pocket. The mutant proteins H206Y and S255F show increased PGE_1 activity in addition to potentiating laurate and arachidonate metabolism above that of wild type. This increased wild-type activity within the SRS2−3 region is believed to be due to a change in the binding pocket volume and surface surrounding substrate-modulating residues. These new binding surfaces are thought to result as a response to our specific site-directed mutations affecting the hydrophobicity and/or charge of neighboring residues lining the binding pocket, thereby altering substrate orientation in the binding pocket. Previous work in the literature characterizing unique amino acids within the active site of CYP2A5, CYP102, CYP101, and CYP11A1 found diminished catalytic activity or altered regiospecificity (*11*) that was proposed to coincide with a change in substrate pocket size. A recent publication of molecular modeling of the CYP4A members, CYP4A1 (rat), CYP4A4 (rabbit), and CYP4A11 (human), with respect to palmitate-bound CYP101 identified differences at the amino acid level and their respective distances from the heme center (*48*). However, the residues identified as unique for CYP4A4 and, therefore, as candidates for possible fatty acid and prostaglandin modulation are shared with CYP4A7. Mutant proteins H206Y, S255F, and H206Y/S255F, but not R90W/W93R, wild-type CYP4A4, or CYP4A7, metabolized arachidonic acid in the absence of cytochrome b_5. These would require the mutation to mimic, albeit to a smaller degree, the conformational influence of cytochrome b_5 docking due to the fact that wild-type CYP4A7 and CYP4A4 are completely cytochrome b_5-dependent for product formation. Attempts to determine a spectral binding constant for cytochrome b_5 were not successful. Potentially, this technique can provide indirect

structural information from the type and affinity of substrate interaction (*49*). For example, cytochrome b_5 could affect the substrate binding pocket through its interaction in different binding modes. However, cytochrome b_5 did not show any optical perturbation of CYP4A7 when examined by optical difference spectroscopy. CPR induced a Type I spectral perturbation of CYP4A7, but not of the mutant protein H206Y. This is indicative of the CPR binding and perturbing the environment of the heme, but not binding directly to the heme. The authors have observed spectral binding constants for the interaction of the primary substrate, laurate, with CYP4A7, in the presence and absence of cytochrome b_5, to be Type I (*18*). It was not possible to determine definitively if this increased activity observed with the mutant proteins H206Y, S255F, and H206Y/S255F is the result of increased binding affinity for cytochrome b_5, CPR, or substrate.

Stopped-flow reduction kinetic experiments comparing wild-type CYP4A7 and the stable mutant protein H206Y showed differences in the rate of flavin reduction. The flavin reduction phase (fast phase) of the monooxygenase reaction of CYP4A7 was not altered in the presence or absence of cytochrome b_5. H206Y displayed a rate reduction at this step when CPR, H206Y, and cytochrome b_5 or apo cytochrome b_5 were complexed. These differences between CYP4A7 and H206Y may reflect mutagenesis-induced changes in the active site pocket that alter monooxygenase component affinity and/or orientation. These data also show a 10-fold increase in the rate of binding between the mutant H206Y and CPR versus wild-type CYP4A7 and CPR (Table 5), indicating an optimization of interaction between the redox partners resulting in an increase in the overall hydroxylation rate by this mutant (Table 3). Since the rates of heme reduction are unchanged, this increase must be due to the stabilization of an active hydroxylation intermediate. Furthermore, mutagenesis-induced changes in the active site pocket may functionally resemble the conformational change seen upon cytochrome b_5 binding to the wild-type CYP4A7. This assumption is based on the parallel between the 3-fold increase in mutant protein substrate hydroxylation and the 10-fold difference in the rate of interaction of CPR with the mutant versus wild-type cytochrome P450 in the presence of cytochrome b_5. There were not significant differences between CYP4A7 and H206Y in cytochrome b_5 interaction rates, although with H206Y the absorbance change upon bindng of cytochrome b_5 did not reach a plateau, indicating that higher concentrations of $Fe^{2+}-CO$ were being generated over time, albeit slowly (Figure 5). This difference is attributed to a less stable H206Y $Fe^{2+}-CO$/cytochrome b_5 complex. This combination of results negates the contribution of cytochrome b_5 as electron donor and supports a conformational modifier role as the cause for the increase in overall substrate hydroxylation activity.

The high degree of amino acid identity among the members of the rabbit CYP4A subfamily (85%) and their characteristic differences in substrate metabolism profiles provide an attractive system for determining structure/function relationships in these P450s. In the absence of more definitive structural data derived from crystals, molecular modeling based on the more primitive fatty acid metabolizer, CYP102, construction of chimeric enzymes, and production of site-directed mutations were used to identify structural properties leading to activity modulation among the substrates (fatty acids, arachidonic acid, and prostaglandins) in these enzymes. While the methods for accomplishing this are established, they have been applied to only a handful of cytochromes P450. Substrate specificity-determining residues remain to be identified from the crystal structures of CYP102 and CYP108. However, as each P450 has its own range of specificity and function, there is a need to characterize each in detail in order to gain an understanding of determinants of function.

REFERENCES

1. Omura, T., and Sato, R. (1964) *J. Biol. Chem. 239*, 2379−2385.
2. Nelson, D. R., Koymans, L., Kamataki, T., Stegeman, J. J., Feyereisen, R., Waxman, D. J., Waterman, M. R., Gotoh, O., Coon, M. J., Estabrook, R. W., Gunsalus, I. C., and Nebert, D. W. (1996) *Pharmacogenetics 6*, 1−42.
3. Johnson, E. F., Walker, D. L., Griffin, K. J., Clark, J. E., Okita, R. T., Muerhoff, A. S., and Masters, B. S. (1990) *Biochemistry 29*, 873−879.
4. Roman, L. J., Palmer, C. N., Clark, J. E., Muerhoff, A. S., Griffin, K. J., Johnson, E. F., and Masters, B. S. (1993) *Arch. Biochem. Biophys. 307*, 57−65.
5. Escalante, B., Falck, J. R., Yadagiri, P., Sun, L. M., and Laniado-Schwartzman, M. (1988) *Biochem. Biophys. Res. Commun. 152*, 1269−1274.
6. Kauser, K., Clark, J. E., Masters, B. S., Ortiz de Montellano, P. R., Ma, Y. H., Harder, D. R., and Roman, R. J. (1991) *Circ. Res. 68*, 1154−1163.
7. Yokotani, N., Bernhardt, R., Sogawa, K., Kusunose, E., Gotoh, O., Kusunose, M., and Fujii-Kuriyama, Y. (1989) *J. Biol. Chem. 264*, 21665−21669.
8. Yokotani, N., Kusunose, E., Sogawa, K., Kawashima, H., Kinosaki, M., Kusunose, M., and Fujii-Kuriyama, Y. (1991) *Eur. J. Biochem. 196*, 531−536.
9. McCabe, T. J. (1998) in *Hormonal Regulation and Localization of Cytochrome P450 of the CYP4A Gene Subfamily*, Ph.D. Dissertation, The University of Texas Health Science Center at San Antonio Graduate School of Biomedical Sciences at San Antonio.
10. Sawamura, A., Kusunose, E., Satouchi, K., and Kusunose, M. (1993) *Biochim. Biophys. Acta 1168*, 30−36.
11. Negishi, M., Iwasaki, M., Juvonen, R. O., Sueyoshi, T., Darden, T. A., and Pedersen, L. G. (1996) *Mutat. Res. 350*, 43−50.
12. Graham-Lorence, S., Truan, G., Peterson, J. A., Falck, J. R., Wei, S., Helvig, C., and Capdevila, J. H. (1997) *J. Biol. Chem. 272*, 1127−1135.
13. Roman, L. J., Clark, J. E., Griffin, K. J., Johnson, E. F., and Masters, B. S. (1992) *FASEB J. 5*, 4593.
14. Gotoh, O. (1992) *J. Biol. Chem. 267*, 83−90.
15. Nishimoto, M., Clark, J. E., and Masters, B. S. (1993) *Biochemistry 32*, 8863−8870.
16. Hosny, G., Roman, L. J., Mostafa, M. H., and Masters, B. S. (1999) *Arch. Biochem. Biophys. 366*, 199−206.
17. Aitken, A. E., Roman, L. J., and Masters, B. S. S. (1997) *FASEB J. 11*, P195.
18. Loughran, P. A., Roman, L. J., Miller, R. T., and Masters, B. S. S. (2000) *Arch. Biochem. Biophys.* (in press).
19. Barnes, H. J., Arlotto, M. P., and Waterman, M. R. (1991) *Proc. Natl. Acad. Sci. U.S.A. 88*, 5597−5601.
20. Roman, L. J., and Masters, B. S. S. (1993) *FASEB J. 7*, 855.
21. Higuchi, R., Krummel, B., and Saiki, R. K. (1988) *Nucleic Acids Res. 16*, 7351−7367.
22. Dayhoff, M. O., Hunter, A. P., and Hunt, L. T. (1983) *Methods Enzymol. 91*, 524−525.
23. Poulos, T. L., Finzel, B. C., Gunsalus, I. C., Wagner, G. C., and Kraut, J. (1985) *J. Biol. Chem. 260*, 16122−16130.
24. Ravichandran, K. G., Boddupalli, S. S., Hasermann, C. A., Peterson, J. A., and Deisenhofer, J. (1993) *Science 261*, 731−736.

25. Hasemann, C. A., Ravichandran, K. G., Peterson, J. A., and Deisenhofer, J. (1994) *J. Mol. Biol. 236*, 1169−1185.
26. Graham, S. E., and Peterson, J. A. (1999) *Arch. Biochem. Biophys. 369*, 24−29.
27. Michael, S. F. (1994) *BioTechniques 16*, 410−412.
28. Roman, L. J., Sheta, E. A., Martásek, P., Gross, S. S., Liu, Q., and Masters, B. S. (1995) *Proc. Natl. Acad. Sci. U.S.A. 92*, 8428−8432.
29. Bradford, M. M. (1976) *Anal. Biochem. 72*, 248−254.
30. Porter, T. D., Wilson, T. E., and Kasper, C. B. (1987) *Arch. Biochem. Biophys. 254*, 353−367.
31. Djordjevic, S., Roberts, D. L., Wang, M., Shea, T., Camitta, M. G., Masters, B. S., and Kim, J. J. (1995) *Proc. Natl. Acad. Sci. U.S.A. 92*, 3214−3218.
32. Holmans, P. L., Shet, M. S., Martin-Wixtrom, C. A., Fisher, C. W., and Estabrook, R. W. (1994) *Arch. Biochem. Biophys. 312*, 554−565.
33. Rogers, M. J., and Strittmatter, P. (1974) *J. Biol. Chem. 249*, 895−900.
34. Cinti, D. L., and Ozols, J. (1975) *Biochim. Biophys. Acta 410*, 32−44.
35. Segel, I. H. (1976) *Biochemical Calculations*, John Wiley & Sons, New York.
36. Yamazaki, H., Johnson, W. W., Ueng, Y. F., Shimada, T., and Guengerich, F. P. (1996) *J. Biol. Chem. 271*, 27438−27444.
37. Guengerich, F. P., and Johnson, W. W. (1997) *Biochemistry 36*, 14741−14750.
38. Miller, R. T., Martásek, P., Omura, T., and Masters, B. S. S. (1999) *Biochem. Biophys. Res. Commun. 265*, 184−188.
39. von Wachenfeldt, C., and Johnson, E. F. (1995) in *Cytochrome P450, Structure and Function* (Ortiz de Montellano, P. R., Ed.) 2nd ed., pp 183−223, Plenum Press, New York.
40. Szklarz, G. D., He, Y. A., and Halpert, J. R. (1995) *Biochemistry 34*, 14312−14322.
41. Szklarz, G. D., He, Y. Q., Kedzie, K. M., Halpert, J. R., and Burnett, V. L. (1996) *Arch. Biochem. Biophys. 327*, 308−318.
42. Szklarz, G. D., and Halpert, J. R. (1997) *J. Comput.-Aided Mol. Des. 11*, 265−272.
43. Shen, S., and Strobel, H. W. (1992) *Arch. Biochem. Biophys. 294*, 83−90.
44. Shen, S., and Strobel, H. W. (1993) *Arch. Biochem. Biophys. 304*, 257−265.
45. Cvrk, T., and Strobel, H. W. (2000) *Arch. Biochem. Biophys.* (in press).
46. Bridges, A., Gruenke, L., Chang, Y. T., Vakser, I. A., Loew, G., and Waskell, L. (1998) *J. Biol. Chem. 273*, 17036−17049.
47. Aitken, A. E., Roman, L. J., and Masters, B. S. S. (1998) *FASEB J. 12*, 656.
48. Lewis, D. F. V., and Lake, B. G. (1999) *Xenobiotica 29*, 763−781.
49. Hoch, U., Falck, J. R., and Ortiz de Montellano, P. R. (2000) *J. Biol. Chem. 275*, 26952−26958.

BI001522U